Synthesis of New 2-Substituted 6-Bromo-3-methylthiazolo[3,2-*a*]-benzimidazole Derivatives and their Biological Activities

Hatem A. Abdel-Aziz[a,*], Nehal A. Hamdy[a], Amira M. Gamal-Eldeen[b,*], and Issa M. I. Fakhr[a]

[a] Applied Organic Chemistry Department, National Research Center, Dokki 12622, Cairo, Egypt. E-mail: hatem_741@yahoo.com
[b] Cancer Biology Laboratory, Center of Excellence for Advanced Sciences, Biochemistry Department, National Research Center, Dokki 12622, Cairo, Egypt. E-mail: aeldeen7@yahoo.com

* Authors for correspondence and reprint requests

Z. Naturforsch. **66c**, 7–16 (2011); received April 9, 2009/August 3, 2010

1-(6-Bromo-3-methyl-1,3-thiazolo[3,2-*a*]benzimidazol-2-yl)ethanone (**2**) was prepared by bromination at ambient temperature of 1-(3-methylthiazolo[3,2-*a*]benzimidazol-2-yl)ethanone (**1**). The structure of **2** was determined by single-crystal X-ray diffraction. The precursor **5** was synthesized by heating a mixture of acetyl **2** and bromine. Various 2-substituted 6-bromo-3-methylthiazolo[3,2-*a*]benzimidazoles containing 1,3-thiazole, 1,4-benzothiazine, quinoxaline or imidazo[1,2-*a*]pyridine moieties were prepared starting from bromoacetyl **5**. Taken together from the biological investigations, **2**, **5**, and **7a** were potent immunosuppressors against both macrophages and T-lymphocytes, and **7b**, **11b**, and **14** were potent immunostimulators towards both types of immune cells. The results also revealed that, among others, **2** and **14** were the most significant inhibitors of LPS-stimulated NO generation, and that **5**, **7a**, and **7b** had a weak radical scavenging activity against DPPH radicals. Moreover, **2**, **5**, and **7a** had a concomitant strong cytotoxicity against colon carcinoma, hepatocellular carcinoma, and lymphoblastic leukemia cells. Collectively, compounds **2**, **5**, and **7a** are multipotent compounds with promising biological activities.

Key words: Anti-Inflammatory, Anticancer, Thiazolo[3,2-*a*]benzimidazole

Introduction

Various substituted thiazolo[3,2-*a*]benzimidazole derivatives are associated with diverse pharmacological activities (Fukunaga *et al*., 2007; Kohara *et al*., 2005). For example, 3-(4-chlorophenyl)thiazolo[3,2-*a*]benzimidazole-2-acetic acid or tilomisole (WY-18,251) was used in the treatment of cancer (Dillman *et al*., 1992) and rheumatoid arthritis besides its benefits as both anti-inflammatory drug (Eickhoff *et al*., 1996) and immunomodulatory agent (Gilman *et al*., 1987). In addition, several 1,3-thiazole (Anandan *et al*., 2007), 1,4-benzothiazine (Schiaffella *et al*., 2006), quinoxaline (Rong *et al*., 2007), and imidazo[1,2-*a*]pyridine (Ismaila *et al*., 2008) derivatives are of significant pharmaceutical importance.

Prompted by these observations and as a continuation of our previous work on the chemistry and biological properties of thiazolo[3,2-*a*]benzimidazole derivatives (Abdel-Aziz *et al*., 2008; Hamdy *et al*., 2007) and the synthesis of biologically active heterocycles (Dawood *et al*., 2005, 2007), we present in this study a novel approach to the synthesis of a battery of compounds starting from the key precursor 2-bromo-1-(6-bromo-3-methylthiazolo[3,2-*a*]benzimidazol-2-yl) ethanone (**5**). These compounds were further screened for their immunomodulatory, anticancer, anti-inflammatory, and antioxidant activities.

Experimental

Chemistry

Melting points were measured with a Gallenkamp apparatus and are uncorrected. IR spectra were recorded on a Shimadzu FT-IR 8101 PC infrared spectrophotometer. The NMR spectra were recorded on a Varian Mercury VX-300 NMR spectrometer. ^{1}H NMR spectra were run at 300 MHz in deuterated dimethylsulfoxide (DMSO-d_6). Chemical shifts are quoted in d and were related to those of the solvents. Mass spectra were measured on a GCMS-QP1000 EX spectrometer at 70 eV. Elemental analyses were

carried out at the Microanalytical Center of Cairo University.

*1-(6-Bromo-3-methyl-1,3-thiazolo[3,2-a]benzimidazol-2-yl)ethanone (**2**)*

A solution of 1-(3-methylthiazolo[3,2-*a*]benzimidazol-2-yl)ethanone (**1**) (2.3 g, 10 mmol) in glacial acetic acid (50 ml) was stirred at ambient temperature, while a bromine solution (1.6 g, 10 mmol) in glacial acetic acid (15 ml) was added drop-wise over a period of 30 min. After the addition was completed, the mixture was stirred at room temperature for further 30 min. The residue that formed was filtered off, washed with acetic acid and dried. Recrystallization from EtOH afforded compound **2** as white needles in 84% yield. – M.p. 203–205 °C. – IR (KBr): ν_{max} = 1648 (C=O), 1604 (C=N) cm^{-1}. – ^1H NMR (DMSO-d_6): δ = 2.62 (s, 3H, CH_3), 3.08 (s, 3H, $COCH_3$), 7.54 (dd, 1H, J = 8.7, 1.8 Hz, ArH of C-7), 7.63 (d, 1H, J = 8.4 Hz, ArH of C-8), 8.23 (d, 1H, J = 1.5 Hz, ArH of C-5). – MS: *m/z* (%) = 312 (6.22) $[M + 3]^+$, 311 (15.97) $[M + 2]^+$, 310 (100) $[M + 1]^+$, 309 (15.19) $[M]^+$, 308 (98.46), 295 (51.06), 220 (53.0), 143 (42.37). – Analysis for $C_{12}H_9BrN_2OS$ (309.19): calcd./found C 46.62/46.38, H 2.93/3.02, N 9.06/9.27, S 10.37/10.13.

*X-ray crystallography of **2***

A single crystal of **2** was obtained by slow evaporation from a mixture of toluene and petroleum ether (40–60). The crystal structure was solved and refined using maXus (Bruker Nonius, Delft, The Netherlands and MacScience, Yokohama, Japan) (Altomare *et al.,* 1994). Mo-Kα radiation (λ = 0.71073 Å) and a graphite monochromator were used for data collection.

Crystal data of **2**: empirical formula, $C_{12}H_9BrN_2OS$; M_r, 309.190; crystal system, monoclinic; space group, *C2/c*; unit cell dimensions, a = 11.4230(6) Å, b = 8.8509(5) Å, c= 23.259(2) Å, β = 103.345(2)°; volume, 2288.0(2) $Å^3$; Z, 8; density, 1.795 mg m^{-3}; θ range for data collection, 2.910–27.485°; absorption coefficient, 3.76 mm^{-1}; T, 298 K; reflections collected, 3946; independent reflections, 2768; observed reflections, 1168; R_{int}, 0.038; R(all), 0.153; wR(ref), 0.129; wR(all), 0.150; S(ref), 4.705; S(all), 3.876; Δ/σ_{max}, 0.043; $\Delta\rho_{max}$, 1.65 e $Å^3$, $\Delta\rho_{min}$, –1.30 e $Å^3$. Crystallographic data for the structure of **2**, reported in this paper, have been deposited with the Cambridge Crystallographic Data Centre (CCDC 675847). Copies of the data can be obtained, free of charge, on application to CCDC, 12 Union Road, Cambridge, CB2 1EZ, UK (Fax: +44-1223-336033 or e-mail: deposit@ccdc.cam.ac.uk).

*2-Bromo-1-(6-bromo-3-methylthiazolo[3,2-a]-benzimidazol-2-yl)ethanone (**5**)*

Method A

A solution of 1-(3-methylthiazolo[3,2-*a*]benzimidazol-2-yl)ethanone (**1**) (2.3 g, 10 mmol) in glacial acetic acid (50 ml) was refluxed while stirring. To the hot solution, a bromine solution (3.2 g, 20 mmol) in glacial acetic acid (25 ml) was added drop-wise over a period of 30 min with stirring; the mixture was maintained at 90–100 °C. After the addition was completed the mixture was stirred vigorously at room temperature for further 1.5 h, till evolution of hydrogen bromide gas ceased and precipitation of the product was completed. Then the solid was filtered off, washed with water and dried. Recrystallization from EtOH/DMF afforded **5** as white powder in 80% yield. – M.p. 265–268 °C. – IR (KBr): ν_{max} = 1654 (C=O), 1603 (C=N) cm^{-1}. – ^1H NMR (DMSO-d_6): δ = 3.06 (s, 3H, CH_3), 4.55 (s, 2H, CH_2), 7.54 (dd, 1H, J = 8.7, 1.8 Hz, ArH of C-7), 7.63 (d, 1H, J = 8.4 Hz, ArH of C-8), 8.22 (d, 1H, J = 1.5 Hz, ArH of C-5). – MS: *m/z* (%) = 391 (4.7) $[M + 3]^+$, 390 (15.0) $[M + 2]^+$, 389 (14.9) $[M + 1]^+$, 388 (22.2) $[M]^+$, 293 (88.9), 295 (100), 232 (27.8), 215 (39.1). – Analysis for $C_{12}H_8Br_2N_2OS$ (388.08): calcd./found C 37.14/37.32, H 2.08/2.15, N 7.22/7.03, S 8.26/8.44.

Method B

This reaction was carried out by the same procedure as described in method A using equimolar quantities of both 1-(6-bromo-3-methyl-1,3-thiazolo[3,2-*a*]benzimidazol-2-yl)ethanone (**2**) and bromine.

*2-(2-Aminothiazol-4-yl)-6-bromo-3-methylthiazolo[3,2-a]benzimidazole (**7a**)*

To a solution of the bromoacetyl derivative **5** (0.39 g, 1 mmol) in absolute ethanol (20 ml), thiourea (**6a**) (0.076 g, 1 mmol) was added. The mixture was refluxed for 5 h, then left to cool. The reaction mixture was treated with a solution of sodium acetate trihydrate till complete precipitation of the product. The solid that formed was

filtered off, washed with water, and dried. Recrystallization from EtOH/DMF afforded the corresponding thiazole derivative **7a** as pale yellow powder in 73% yield. – M.p. >300 °C. – IR (KBr): ν_{max} = 3289, 3136 (NH_2), 1636 (C=N) cm^{-1}. – ^1H NMR (DMSO-d_6): δ = 2.89 (s, 3H, CH_3), 6.91 (s, 1H, CH of thiazole), 6.99 (s, 1H, NH_2, D_2O exchangeable), 7.49 (dd, 1H, J = 8.7, 1.8 Hz, ArH of C-7), 7.63 (d, 1H, J = 8.4 Hz, ArH of C-8), 8.15 (d, 1H, J = 1.5 Hz, ArH of C-5). – MS: *m/z* (%) = 368 (10.44) $[M + 4]^+$, 367 (17.79) $[M + 3]^+$, 366 (100) $[M + 2]^+$, 365 (18.62) $[M + 1]^+$, 364 (95.54) $[M]^+$, 286 (66.95), 69 (86.08), 60 (92.22). – Analysis for $C_{13}H_9BrN_4S_2$ (363.95): calcd./found C 42.75/42.91, H 2.48/2.29, N 15.34/15.16, S 17.56/17.48.

*6-Bromo-2-(2-cyanomethylthiazol-4-yl)-3-methylthiazolo[3,2-a]benzimidazole (**7b**)*

To a solution of the bromoacetyl derivative **5** (0.39 g, 1 mmol) in absolute ethanol (20 ml), cyanothioacetamide (**6b**) (0.10 g, 1 mmol) was added. The mixture was refluxed for 7 h. The solid that formed was filtered off, washed with ethanol, and dried. Recrystallization from EtOH/DMF afforded the corresponding thiazole derivative **7b** as pale brown fine needles in 78% yield. – M.p. >300 °C. – IR (KBr): ν_{max} = 2256 (C≡N), 1611 (C=N) cm^{-1}. – ^1H NMR (DMSO-d_6): δ = 3.04 (s, 3H, CH_3), 4.67 (s, 2H, CH_2), 7.49 (dd, 1H, J = 8.7, 1.8 Hz, ArH of C-7), 7.64 (d, 1H, J = 8.4 Hz, ArH of C-7), 8.04 (s, 1H, CH of thiazole), 8.23 (d, 1H, J = 1.5 Hz, ArH of C-5). – MS: *m/z* (%) = 392 (4.56) $[M + 3]^+$, 391 (14.9) $[M + 2]^+$, 390 (80.8) $[M + 1]^+$, 389 (13.1) $[M]^+$, 310 (55.4), 243 (20.8), 111 (28.5), 97 (53.8), 83 (71.5), 55 (100). –Analysis for $C_{15}H_9BrN_4S_2$ (389.29): calcd./found C 46.28/46.43, H 2.33/2.37, N 14.39/14.48, S 16.47/16.25.

*General procedure for the reaction of **5** with o-aminothiophenol, o-phenylenediamine and 2-aminopyridine*

A mixture of the bromoacetyl derivative **5** (0.39 g, 1.0 mmol) and *o*-aminothiophenol, *o*-phenylenediamine or 2-aminopyridine (1.0 mmol) in ethanol (30 ml) was refluxed for 4 h. The solid that formed was filtered off, washed with ethanol, and dried. Recrystallization from DMF/H_2O afforded the corresponding fused compounds **11a**, **11b**, and **14**, respectively.

*2-(2H-1,4-Benzothiazin-3-yl)-6-bromo-3-methylthiazolo[3,2-a]benzimidazole (**11a**)*

Yellow fine needles; yield, 66%. – M.p. >300 °C. – IR (KBr) ν_{max} = 1606 (C=N) cm^{-1}. – ^1H NMR (DMSO-d_6): δ = 3.08 (s, 3H, CH_3), 3.97 (s, 2H, CH_2, C-2 of benzothiazine), 7.19–7.66 (m, 6H, ArH), 8.24 (d, 1H, J = 1.5 Hz, ArH of C-5 in thiazolobenzimidazole). – MS: *m/z* (%) = 417 (7.73) $[M + 3]^+$, 416 (12.59) $[M + 2]^+$, 415 (63.66) $[M + 1]^+$, 414 (18.03) $[M]^+$, 413 (69.96), 186 (93.28), 120 (100), 68 (91.56). – Analysis for $C_{18}H_{12}BrN_3S_2$ (414.34): calcd./found C 52.18/52.41, H 2.92/2.87, N 10.14/9.99, S 15.48/15.20.

*6-Bromo-2-(quinoxalin-2-yl)-3-methylthiazolo[3,2-a]benzimidazole (**11b**)*

Yellow crystals; yield, 66%. – M.p. >300 °C. – IR (KBr): ν_{max} = 1609 (C=N) cm^{-1}. – ^1H NMR (DMSO-d_6): δ = 3.22 (s, 3H, CH_3), 7.52–8.15 (m, 6H, ArH), 8.29 (d, 1H, J = 1.5 Hz, ArH of C-5 in thiazolobenzimidazole), 9.4 (s, 1H, H of C-3 in quinoxaline). – MS: *m/z* (%) = 397 (9.98) $[M + 2]^+$, 396 (3.05) $[M + 1]^+$, 395 (4.07) $[M]^+$, 76 (100), 63 (38.29). – Analysis for $C_{18}H_{11}BrN_4S$ (395.28): calcd./found C 54.69/54.47, H 2.80/2.93, N 14.17/14.02, S 8.11/8.22.

*6-Bromo-2-imidazo[1,2-a]pyridin-2-yl-3-methylthiazolo[3,2-a]benzimidazole (**14**)*

White powder; yield, 68%. – M.p. >300 °C. – IR (KBr) ν_{max} = 1623 (C=N) cm^{-1}. – ^1H NMR (DMSO-d_6): δ = 3.04 (s, 3H, CH_3), 6.95–7.65 (m, 5H, ArH), 8.22 (d, 1H, J = 1.5 Hz, ArH of C-5 in thiazolobenzimidazole), 8.44 (s, 1H, imidazole), 8.54 (d, 1H, J = 6.0 Hz, ArH of C-5 in pyridine). – MS: *m/z* (%) = 385 (9.56) $[M + 2]^+$, 384 (36.36) $[M + 1]^+$, 383 (14.69) $[M]^+$, 382 (31.47), 155 (41.72), 77 (100). – Analysis for $C_{17}H_{11}BrN_4S$ (383.27): calcd./found C 53.27/53.06, H 2.89/2.77, N 14.62/14.64, S 8.37/8.24.

Biological activity assays

Cell culture

Several human cell lines were used in testing the anticancer activity including: lymphoblastic leukemia (1301 cells; a generous gift from The Training Center of DakoCytomation, Elly, UK), hepatocellular carcinoma (Hep-G2), colon carcinoma (HCT-116), and Raw murine macrophage (RAW 264.7) (ATCC, VA, USA). Cells were routinely

cultured in DMEM (Dulbeco's modified Eagle's medium), except for RAW 264.7 cells, which were grown in RPMI-1640 medium at 37 °C in humidified air containing 5% CO_2. Media were supplemented with 10% fetal bovine serum (FBS), 2 mM L-glutamine, containing 100 units/ml penicillin G sodium, 100 units/ml streptomycine sulfate, and 250 ng/ml amphotericin B. Monolayer cells were harvested by trypsin/EDTA treatment, except for RAW 264.7 cells, which were collected by gentle scraping. The tested compounds were dissolved in dimethyl sulfoxide (DMSO, 99.9%, HPLC grade) and diluted 1000-fold in the assay solutions. In all cellular experiments, results were compared with DMSO-treated cells. Compound dilutions were tested before assays for endotoxin using the Pyrogent® Ultra gel clot assay, and they were found to be endotoxin-free. All experiments were repeated four times, unless otherwise mentioned, and the data was represented as mean ± S.D. Unless otherwise mentioned, cell culture material was obtained from Cambrex BioScience (Copenhagen, Denmark), and all chemicals were from Sigma (St. Louis, MO, USA).

Proliferation of immune cells

The effect of the synthesized compounds on the growth of Raw murine macrophages 264.7 and 1301 cells (T-lymphocytes) was estimated by the 3-(4,5-dimethyl-2-thiazolyl)-2,5-diphenyl-2*H*-tetrazolium bromide (MTT) assay (Hansen *et al*., 1989). The yellow tetrazolium salt of MTT is reduced by mitochondrial dehydrogenases in metabolically active cells to form insoluble purple formazan crystals, which are solubilized by the addition of a detergent. Cells ($5 \cdot 10^4$ cells/well) were incubated with various concentrations of the compounds at 37 °C in a FBS-free medium, before submitted to the MTT assay. The absorbance was measured with an ELISA reader (Bio-Rad, Munich, Germany) at 570 nm. The relative cell viability was determined by the amount of MTT converted to the insoluble formazan salt. The data are expressed as the mean percentage of viable cells as compared to DMSO-treated cells. Treatment of macrophages with 1000 U/ml recombinant macrophage colony-stimulating factor (M-CSF, Pierce, USA) was used as positive control.

Nitrite assay

The accumulation of nitrite, an indicator of NO synthesis, was measured using the Griess reagent (Gerhäuser *et al*., 2003). RAW 264.7 cells were grown in phenol red-free RPMI-1640 medium containing 10% FBS. Cells were incubated for 24 h with lipopolysaccharide (LPS) (1 μg/ml) in the presence or absence of the test compounds (12.5 and 25 μg/ml). 50 μl of cell culture supernatant were mixed with 50 μl of Griess reagent and incubated for 10 min. The absorbance was measured spectrophotometrically at 550 nm. A standard curve was plotted using serial concentrations of sodium nitrite. The nitrite content was normalized to the cellular protein content as measured by the bicinchoninic acid assay (Smith *et al*., 1992).

The percentage of NO inhibition was calculated by submitting the nitrite contents of the cell supernatants of cultures treated with DMSO (control), LPS, or LPS/test compounds to the following equation: % NO inhibition = $(\text{nitrite}_{\text{compound}} - \text{nitrite}_{\text{control}})/(\text{nitrite}_{\text{LPS}} - \text{nitrite}_{\text{control}}) \cdot 100$.

Cytotoxicity assay

The effect of the test compounds on the growth of hepatocellular carcinoma (Hep-G2) and colon carcinoma (HCT-116) cells, respectively, was estimated by the MTT assay. The relative cell viability was expressed as the mean percentage of viable cells compared to the respective DMSO-treated cells (control). The half maximal growth inhibitory concentration, IC_{50} value, was calculated from the line equation of the dose-response curve of each compound. The results were compared with the cytotoxic activity of paclitaxel, a known anticancer drug, against both cell lines.

Antioxidant assay

The antioxidant capacity of the test compounds was studied through their scavenging activity against 1,1-diphenyl-2-picryl-hydrazyl (DPPH) radicals (Van Amsterdam *et al*., 1992; Gerhäuser *et al*., 2003). The bleaching of DPPH was monitored by the absorbance at 515 nm. The percentage of DPPH bleaching utilized for SC_{50} (half maximal scavenging concentration) was calculated as follows: 0% is the absorbance of DPPH and 100% is the absorbance of DPPH with an efficient scavenger (10 mM ascorbic acid, AA).

Statistical analysis

MTT assay data were analysed using two-factorial analysis of variance (ANOVA), including first-order interactions (two-way ANOVA), followed by the Tukey post hoc test for multiple comparisons. Other test data were analysed using

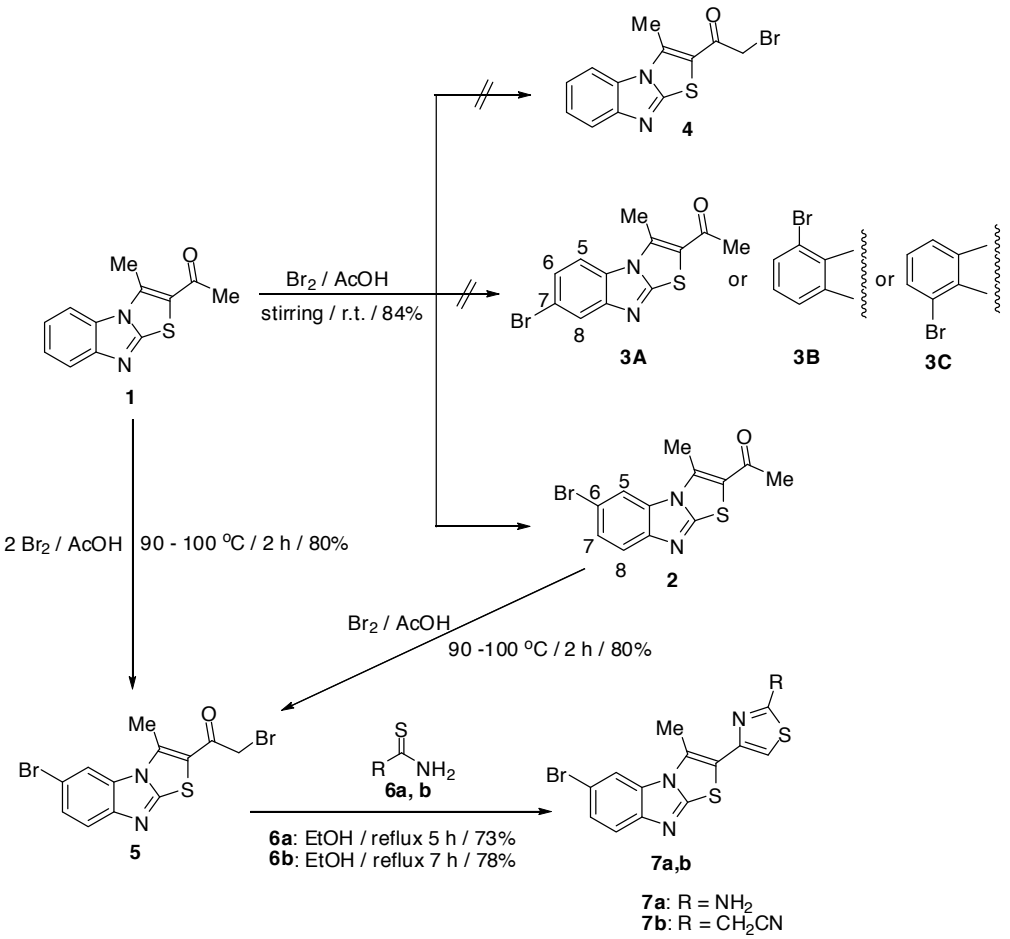

Scheme 1. Synthetic route to compounds **2**, **5**, **7a**, and **7b**.

one-way ANOVA followed by the Tukey post hoc test. $P < 0.05$ indicated statistical significance.

Results and Discussion

Chemistry

The starting material 1-(3-methylthiazolo[3,2-*a*]benzimidazol-2-yl)ethanone (**1**) was prepared according to a previously reported method (D'Amico *et al*., 1964). The hitherto unreported 1-(6-bromo-3-methyl-1,3-thiazolo[3,2-*a*]benzimidazol-2-yl)ethanone (**2**) was prepared by the treatment of **1** with bromine in acetic acid at ambient temperature to afford a single product for which structures **2**, **3A**, **3B**, **3C** or **4** seemed possible (Scheme 1).

The ^{1}H NMR spectrum of the isolated product revealed the singlet signal of the acetyl function at δ 3.08 ppm in addition to the pattern of 1,2,4-substituted benzene, represented as one doublet of doublet signal and two doublets in the aromatic region at δ 7.54 (dd, 1H, J = 8.7, 1.8 Hz, ArH), 7.63 (d, 1H, J = 8.4 Hz, ArH) and 8.23 ppm (d, 1H, J = 1.5 Hz, ArH). These findings ruled out the other possible structure **4**, and also excluded the possibilities of bromination at C-5 or C-8 (1,2,3-substituted benzene pattern), which are represented by structures **3B** and **3C**, respectively, but not enough to exclude the structure **3A**, where bromination may take place at C-7. However, the structure **2** was assigned for the reaction product on the basis of its single-crystal X-ray diffraction pattern (Fig. 1).

We found that, the reaction of **1**, using two molar equivalents of bromine in acetic acid at 90–100 °C, resulted in the corresponding bro-

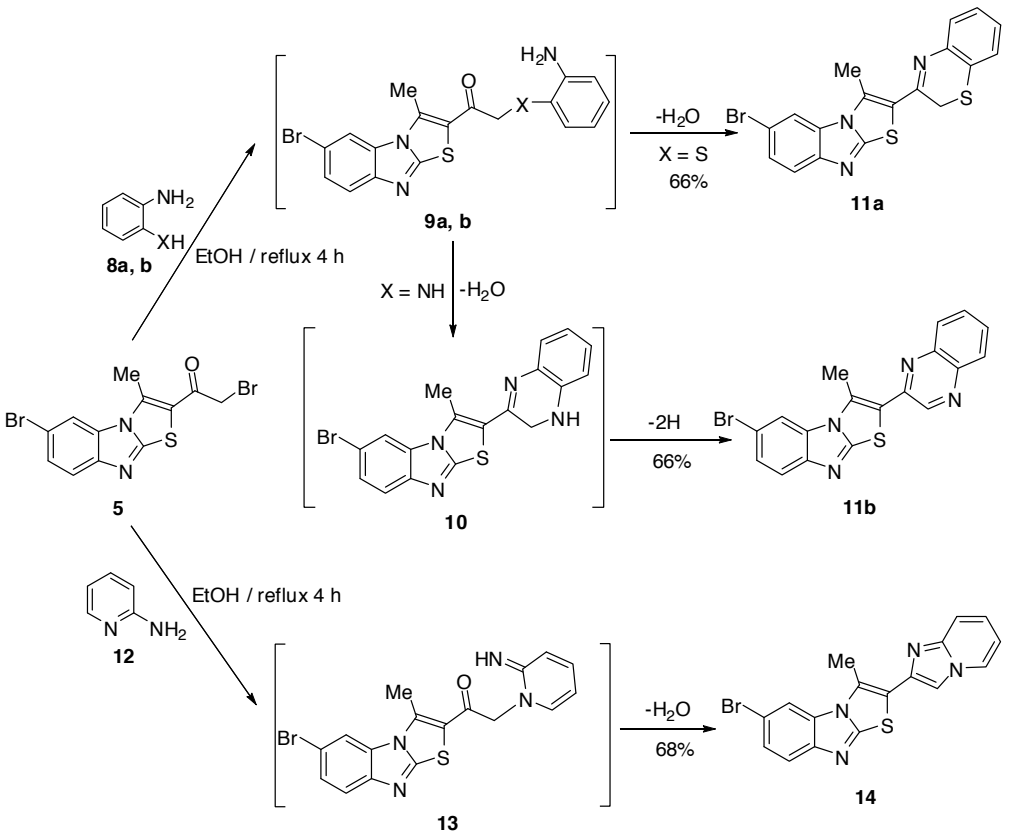

Scheme 2. Synthetic route to compounds **11a**, **11b**, and **14**.

moacetyl derivative **5**. Its ^{1}H NMR spectrum revealed the singlet signal of integral to two protons of a methylene group at δ 4.55 ppm and the signals of three aromatic protons at δ 7.54, 7.63 and 8.22 ppm corresponding to C-7, C-8 and C-5, respectively. Its mass spectrum showed a peak corresponding to its molecular ion at *m/z* 388 [M$^+$] (Scheme 1). The structure of **5** was further confirmed by an independent synthesis outlined in Scheme 1. Thus, treatment of **2** with equal molar quantity of bromine in acetic acid at 90–100 °C resulted in the formation of a product identical to **5**.

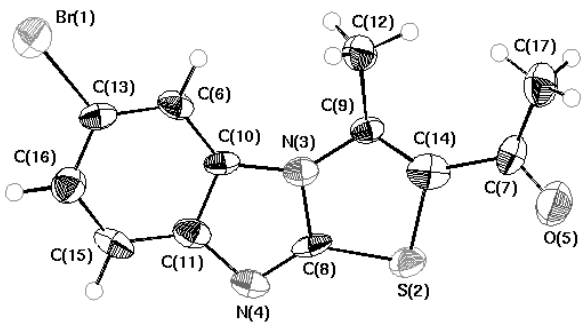

Fig. 1. The X-ray structure of compound **2**.

The reaction of compound **5** with thiourea in refluxing ethanol afforded the corresponding 1,3-thiazole derivative **7a**. The structure of the product was elucidated on the basis of its elemental analysis and spectral data. Its IR spectum revealed the appearance of two absorption bands at 3289 and 3136 cm^{-1} corresponding to the amino function and showed no carbonyl absorption band in the region 1600–1750 cm^{-1}. The ^{1}H NMR spectrum of **7a** showed the appearance of the thiazole proton singlet signal at δ 6.91 ppm and a D_2O exchangeable broad signal of the NH_2 group at δ 6.99 ppm [cf. Experimental] (Scheme 1).

Afterwards, the reaction of **5** with cyanothioacetamide **6a** in refluxing ethanol furnished the cyanomethyl derivative **7b**. The IR spectum of

7b showed an absorption band at 2256 cm^{-1} corresponding to the nitrile function, whereas its ^1H NMR spectrum showed the appearance of a singlet signal of the methylene proton at δ 4.67 ppm and its mass spectrum revealed a peak corresponding to the molecular ion.

When the bromoacetyl derivative **5** was treated with *o*-aminothiophenol in refluxing ethanol, it afforded a yellow crystalline product identified as 2-(2*H*-1,4-benzothiazin-3-yl)-6-bromo-3-methylthiazolo[3,2-*a*]benzimidazole (**11a**). Its ^1H NMR spectrum displayed a singlet at δ 3.97 ppm assignable to the two protons of the methylene group in addition to the multiplet signal of seven aromatic protons in the aromatic region. A plausible mechanism for the formation of the 1,4-benzothiazine derivative **11a** is depicted in Scheme 2.

Similarly, **5** reacted with *o*-phenylenediamine to afford the quinoxaline derivative **11b**. The structure of the latter product was established from its spectral data, which exclude the other possible structure of the intermediate **10**. The IR spectrum of **11b** showed the absence of the NH band in the region 3400–3100 cm^{-1}, whereas the ^1H NMR spectrum of **11b** revealed the characteristic singlet signal due to the proton of C-3 in the quinoxaline moiety at δ 9.4 ppm. A reasonable mechanism for the formation of the product **11b** through oxidation of the non-isolable intermediate **10** during the course of the reaction is outlined in Scheme 2.

Furthermore, treatment of **5** with 2-aminopyridine in refluxing ethanol afforded only one isolable product (as examined by TLC). The structure of the isolated product was identified as 6-bromo-2-imidazo[1,2-*a*]pyridin-2-yl-3-methylthiazolo[3,2-*a*]benzimidazole (**14**). Its ^1H NMR showed the characteristic singlet of C-3 in the imidazolylpyridine moiety at δ 8.44 ppm, and its mass spectrum revealed a peak corresponding to the molecular ion. The formation of **14** can be explained on the basis of an initial substitution at the ring nitrogen of 2-aminopyridine with α-bromo ketone **5** (Adams and Dix, 1958) to afford the non-isolable intermediate **13**. The latter intermediate underwent cyclization into the imidazopyridine derivative **14** *via* the loss of a water molecule (Scheme 2).

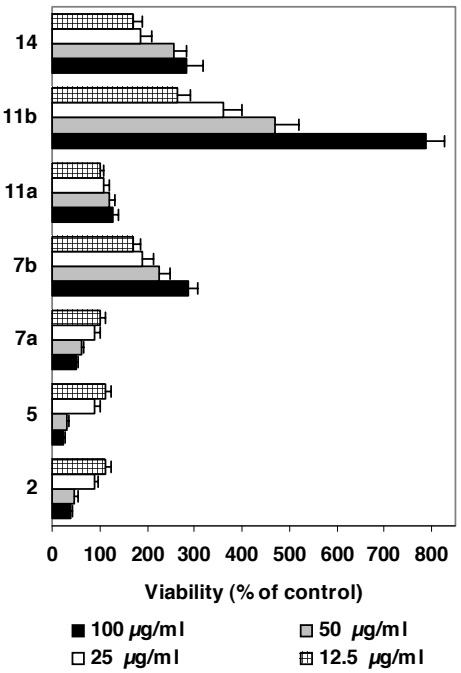

Fig. 2. The effect of different doses of the compounds **2**, **5**, **7a**, **7b**, **11a**, **11b**, and **14** on the growth of Raw murine macrophages 264.7, as measured by the MTT assay. The viability results are represented as the percentage of control cells (mean ± S.D., $n = 4$).

Screening of biological activities

Macrophages are the first line of defense in innate immunity against microbial infection. Phagocytes engulf and kill microorganisms and present antigens for triggering adaptive immune responses (Girotti *et al*., 2004). Accordingly, the induction of macrophage proliferation is crucial in the assessment of innate immunity. The treatment with the compounds **2**, **5**, **7a**, **7b**, **11a**, **11b**, and **14** indicated that **7b** is a significant stimulator of macrophage growth starting from the lowest tested dose (12.5 μg/ml) with 1.7-fold growth referring to control ($P < 0.05$) going to the highest tested dose (100 μg/ml) with 2.9-fold growth referring to control ($P < 0.01$), compared with DMSO-treated cells (Fig. 2). Surprisingly, **2**, **5**, and **7a** were strong suppressors of macrophage proliferation (Fig. 2), as indicated by their IC_{50} values of 74.06, 61.44, and 89.15 μg/ml, respectively.

We further investigated whether the proliferative activity of most of the test compounds is specific for macrophages only or towards other immune cells also, so we tested their effect on the growth of T-lymphocytes (lymphoblastic leukemia 1301 cell line). Our findings indicated that **7b**, **11b**, and **14** were strong dose-dependent in-

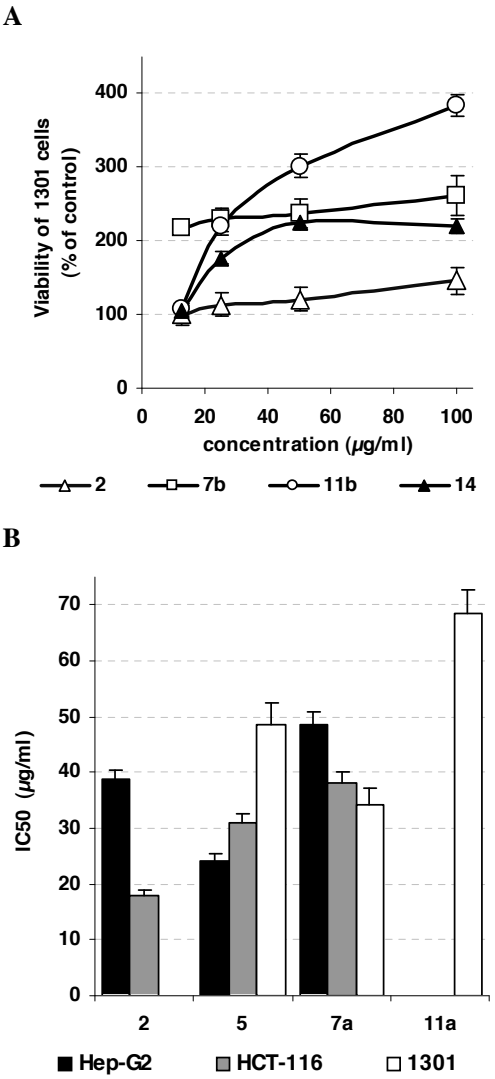

Fig. 3. (A) The stimulatory effect of different compound doses on the growth of 1301 cells. (B) The IC_{50} values (in μg/ml) of the cytotoxic compounds against Hep-G2 cells, HCT-116 cells, and 1301 cells, as measured by the MTT assay. The results are represented as means ± S.D., $n = 4$.

ducers of the T-lymphocytes growth, but among them, **11b** was a dramatic inducer at the tested doses (25–100 μg/ml, $P < 0.001$), and the others produced a low slope in the growth curve with increasing doses (Fig. 3A). Compounds **5**, **7a**, and **11a** were cytotoxic against T-lymphocytes, and their calculated IC_{50} values are shown in Fig. 3B, where the most cytotoxic compounds were **7a** and **5**. From these findings it is obvious that **2**, **5**, and **7a** were strong immunosuppressors (immunotoxic compounds) against both macrophages and T-lymphocytes, and that, among the growth stimulators, compounds **7b**, **11b**, and **14** were the strongest immunostimulators (immunoproliferative) towards both macrophages and T-lymphocytes. This fast growth within 24 h may be due to a real induction of cell growth through enhancement of DNA synthesis, cell cycle, and/or correlated growth factors such as IL-12 for macrophages and IL-2 for lymphocytes. However, it may be also due to total elevation in the intracellular metabolism, especially mitochondrial dehydrogenases. The effect of the test compounds on the proliferation of macrophages and T-lymphocytes suggested that the skeleton of the bromomethyl thiazolo[3,2-*a*]-benzimidazole structure was responsible for the immunotoxicity of **2**, **5**, and **7a** against both types of cells, and that only the substitution with the cyanomethyl moiety in the thiazole derivative converted this toxicity into a strong growth stimulatory potency of **7b**.

On the other hand, the compounds derived from the immunotoxic bromoacetyl derivative **5** exhibited different effects on the growth of immune cells. Although the benzothiazine derivative **11a** possessed a marginal cytotoxicity against 1301 cells, the quinoxaline derivative **11b** had a dramatic growth stimulatory effect on both types of immune cells, and the imidazopyridine derivative **14** showed also low growth stimulation of both cell lines.

For exploring the cytotoxic effect of the test compounds on cancer cell lines, Hep-G2 and HCT-116 cells were treated with different doses of the compounds, and then subjected to the MTT assay. The experiment showed that most of the compounds had no effect on the growth of both types of cells, except **2**, **5**, and **7a**, which exhibited a concomitant strong cytotoxic effect on both types of cells as indicated by their IC_{50} values in Fig. 3b. The most remarkable cytotoxic compounds against Hep-G2, HCT-116, and 1301 cells were **5**, **2**, and **7a**, respectively. Paclitaxel, the known anticancer agent, was found to have an IC_{50} value of 660 ng/ml against Hep-G2 cells and 915 ng/ml against HCT-116 cells.

These findings suggested that the skeleton of the bromomethyl thiazolo[3,2-*a*]benzimidazole structure was responsible for the cytotoxicity of **2**, **5**, and **7a** against both types of solid tumour cells, and that only the substitution with cyanome-

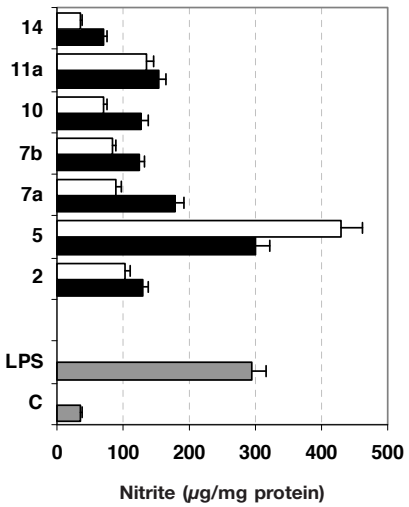

Fig. 4. The anti-inflammatory activity of two doses (12.5 μg/ml as black bars, and 25 μg/ml as white bars) of the synthesized compounds **2**, **5**, **7a**, **7b**, **10**, **11a**, and **14** on NO generation from LPS-stimulated macrophages, in comparison with LPS-treated and untreated (C) macrophages (grey bars). The nitrite concentration, as an index of NO generation, was measured by the Griess assay (mean ± S.D., $n = 4$).

thyl in the thiazole derivative **7b** suppresses this toxicity. On the other hand, it seems that the substitution with benzothiazine in **11a**, quinoxaline in **11b**, or imidazopyridine in **14** in the cytotoxic bromoacetyl derivative **5** resulted in an efficient suppression of its cytotoxicity against hepatic and colon carcinoma cells.

In the inflammation process many mediators are involved including cytokine secretion and nitric oxide (NO) (MacMicking *et al.*, 1997). NO is a highly reactive free radical, and it can form a number of oxidation products (Girotti *et al.*, 2004). In inflammatory diseases, NO is produced in large quantities by the action of inducible NO synthase (iNOS) and cyclooxygenase-2 (COX-2) (Hu *et al.*, 1992), leading to inflammatory consequences and persistent pain.

As a mimic *in vitro* model of inflammation, macrophages were stimulated by incubation with the bacterial lipopolysaccharide (LPS), which activates the macrophage functions and the release of inflammatory mediators including the enhancement of iNOS, the generation of NO, and the secretion of the pro-inflammatory cytokines. Since most of the cellular generated NO is converted immediately into nitrite, RAW 264.7 cells were stimulated with LPS and the nitrite levels were measured in cell culture supernatants before and after the treatment with safe doses of 12.5 and 25 μg/ml of each compound.

The treatment with **5** led to a dramatic increment in the generation of NO, higher than the LPS-stimulated NO generation (Fig. 4), while the other compounds inhibited LPS-stimulated NO generation to various degrees, ranging from 14.5% to 88.2% at 25 μg/ml (Fig. 4). The results also revealed that **14** was the most significant inhibitor of LPS-stimulated NO generation at both tested doses with inhibition ranging from 56.0% to 88.2% ($P < 0.05$) (Fig. 4), which suggested a potential anti-inflammatory activity.

The inhibition of NO may be due to a direct scavenging of NO, inhibition of the iNOS pathway, and/or a modulation of other factors in the NO cascade such as transcriptional factors. Investigation of the radical scavenging activity by the DPPH assay revealed that none of the compounds had radical scavenging activity at the tested concentrations, <100 μg/ml, except **5**, **7a**, and **7b** with calculated SC_{50} values of 95.4, 97.0, and 84.2 μg/ml, respectively, *i.e.* they are weak antioxidants compared with ascorbic acid (SC_{50} 8.6 μg/ml). These findings suggested that the NO inhibition was not due to direct scavenging of NO, but rather due to the inhibition of the iNOS cascade.

The effect of the test compounds on NO generation from macrophages suggested that the skeleton of the bromomethyl thiazolo[3,2-*a*]benzimidazole structure was responsible for the strong inhibition, however, it seems that the substitution with the bromoacetyl moiety in **5** converted this activity into a potential induction of the NO generation from macrophages. This induction may be due to a high induction of the expression on iNOS by this dibromo compound. On the other hand, substitution with imidazopyridine in **14** may lead to the highest inhibition of the iNOS pathway that may lead to its strong inhibition of NO.

Acknowledgement

This work was financially supported by National Research Center, Cairo, Egypt.

Abdel-Aziz H. A., Hamdy N. A., Farag A. M., and Fakhr I. M. I. (2008), Synthesis of some novel pyrazolo[1,5-*a*]pyrimidine, 1,2,4-triazolo[1,5-*a*]pyrimidine, pyrido[2,3-*d*]pyrimidine, pyrazolo[5,1-*c*]-1,2,4-triazine and 1,2,4-triazolo[5,1-*c*]-1,2,4-triazine derivatives incorporating a thiazolo[3,2-*a*]benzimidazole moiety. J. Heterocycl. Chem. **45**, 1–5.

Adams R. and Dix J. S. (1958), The reaction of 2-aminopyridine with α-halo ketones. J. Am. Chem. Soc. **80**, 4618–4620.

Altomare A., Cascarano G., Giacovazzo C., Guagliardi A., Burla M. C., Polidori G., and Camalli M. (1994), Program for automatic solution of crystal structures by direct methods optimized for powder data. J. Appl. Cryst. **27**, 435–436.

Anandan S., Ward J. S., Brokx R. D., Denny T., Bray M. R., Patel D. V., and Xiao X. (2007), Design and synthesis of thiazole-5-hydroxamic acids as novel histone deacetylase inhibitors. Bioorg. Med. Chem. Lett. **17**, 5995–5999.

D'Amico J. J., Campbell R. H., and Guinn E. C. (1964), Derivatives of 3-methylthiazolo[3,2-*a*]benzimidazole. J. Org. Chem. **29**, 865–869.

Dawood K. M., Farag A. M., and Abdel-Aziz H. A. (2005), Azoles and azolo-azines *via* 3-(3-methylbenzofuran-2-yl)-3-oxopropanenitrile. J. Chem. Res., 378–381.

Dawood K. M., Farag A. M., and Abdel-Aziz H. A. (2007), Synthesis of some new benzofuran-based thiophene, 1,3-oxathiole and 1,3,4-oxa(thia)diazole derivatives. Heteroatom Chem. **18**, 294–300.

Dillman R. O., Ryan K. P., Dillman J. B., Shawler D. L., and Maguire R. (1992), Phase I cancer trials: limitations and implications. Mol. Biother. **4**, 10–14.

Eickhoff W. M., Engers D. A., and Mueller K. R. (1996), Nanoparticulate nsaid compositions. U.S. patent **96**, 24, 336.

Fukunaga I., Yeo C. H., and Batchelor A. M. (2007), Potent and specific action of the mGlu1 antagonists YM-298198 and JNJ16259685 on synaptic transmission in rat cerebellar slices. Br. J. Pharmacol. **151**, 870–876.

Gerhäuser C., Klimo K., Heiss E., Neumann I., Gamal-Eldeen A., Knauft J., Liu J.-U., Sitthimonchai S., and Frank N. (2003), Mechanism-based *in vitro* screening of potential cancer chemopreventive agents. Mutat. Res. **523–524**, 163–172.

Gilman S. C., Carlson R. P., Daniels J. F., Datko L., Berner P. R., Chang J., and Lewis A. J., (1987), Immunological abnormalities in rats with adjuvant-induced arthritis – II. Effect of antiarthritic therapy on immune function in relation to disease development. Int. J. Immunopharmacol. **9**, 9–16.

Girotti M., Evans J. H., Burke D., and Leslie C. C. (2004), Cytosolic phospholipase A2 translocates to forming phagosomes during phagocytosis of zymosan in macrophages. J. Biol. Chem. **279**, 19113–19121.

Hamdy N. A., Abdel-Aziz H. A., Farag A. M., and Fakhr I. M. I. (2007), Synthesis of some 1,3-thiazole, 1,3,4-thiadiazole, pyrazolo[5,1-*c*]-1,2,4-triazine, and 1,2,4-triazolo[5,1-*c*]-1,2,4-triazine derivatives based on the thiazolo[3,2-*a*]benzimidazole moiety. Monatsh. Chem. **138**, 1001–1010.

Hansen M. B., Nielsen S. E., and Berg K. (1989), Re-examination and further development of a precise and rapid dye method for measuring cell growth/cell kill. J. Immunol. Methods **119**, 203–210.

Hu L., Gunn C., and Beckman J. (1992), Bactericidal activity of peroxynitrite. Arch. Biochem. Biophys. **298**, 452–457.

Ismaila M. A., Arafa R. K., Wenzler T., Brun R., Tanious F. A., Wilson W. D., and Boykin D. W. (2008), Synthesis and antiprotozoal activity of novel bis-benzamidino imidazo[1,2-*a*]pyridines and 5,6,7,8-tetrahydro-imidazo[1,2-*a*]pyridines. Bioorg. Med. Chem. **16**, 683–691.

Kohara A., Toya T., Tamura S., Watabiki T., Nagakura Y., Shitaka Y., Hayashibe S., Kawabata S., and Okada M. (2005), Radioligand binding properties and pharmacological characterization of 6-amino-*N*-cyclohexyl-*N*,3-dimethylthiazolo[3,2-*a*]benzimidazole-2-carboxamide (YM-298198), a high-affinity, selective, and noncompetitive antagonist of metabotropic glutamate receptor type 1. J. Pharmacol. Exp. Ther. **315**, 163–169.

MacMicking J., Xie Q. W., and Nathan C. (1997), Nitric oxide and macrophage function. Annu. Rev. Immunol. **15**, 323–350.

Rong F., Chow S., Yan S., Larson G., Hong Z., and Wu J. (2007), Structure-activity relationship (SAR) studies of quinoxalines as novel HCV NS5B RNA-dependent RNA polymerase inhibitors. Bioorg. Med. Chem. Lett. **17**, 1663–1666.

Schiaffella F., Macchiarulo A., Milanese L., Vecchiarelli A., and Fringuelli R. (2006), Novel ketoconazole analogues based on the replacement of 2,4-dichlorophenyl group with 1,4-benzothiazine moiety: design, synthesis, and microbiological evaluation. Bioorg. Med. Chem. **14**, 5196–5203.

Smith R., Krohn P. K., Hermanson G. T., Mallia A. K., Gartner F. H., Provenzano M. D., Fujimoto E. K., Goeke N. M., Olson B. J., and Klenk D. C. (1992), Measurement of protein using bicinchoninic acid. Anal. Biochem. **150**, 76–80.

Van Amsterdam F. T., Roveri A., Maiorino M., Ratti E., and Ursini F. (1992), Lacidipine: A dihydropyridine calcium antagonist with antioxidant activity. Free Rad. Biol. Med. **12**, 183–187.